Power Consumption for Core Scraping in the Separation of Rind-Pith from Corn Stalk

Zhengguang Chen [a] and Defu Wang [b,*]

In order to study the energy consumption of separation of pith and rind of corn stalk, a self-designed corn stalk separating unit was adopted in this work to measure the energy consumption by an electric power method. Four parameters—the rotational speed of pith-stripping, clearance between teeth and panel, feeding speed of stalk, and helix angle—were selected as influencing factors. By choosing the three indicators, effective specific energy (ESE), total specific energy (TSE), and energy utilization ratio (EUR) as evaluation indexes, response surface analysis was employed to obtain the influence law model of various experimental factors on evaluation indexes based on orthogonal tests. After all evaluation indexes, working efficiencies, and stalk scraping effects were taken into a comprehensive consideration, the working parameters of the core scraping mechanism were selected as follows: 840 r/min for the rotational speed of pith-stripping, 413 r/min for the feeding speed, 1.56 mm for the tooth-panel clearance, and 25° for the helix angle of scrapper blade. In this case, ESE, TSE, and EUR were 2.21 Wh·kg^{-1}, 10.73 Wh·kg^{-1}, and 22.29%, respectively. The results could be applied to the design and optimization of separation of pith and rind of corn stalk.

Keywords: Corn Stalk; Rind-Pith Separation; Effective Specific Energy; Total Specific Energy

*Contact information: a: College of Information Science & Technology, Heilongjiang Bayi Agricultural University, Daqing, Heilongjiang 163319, China; b: College of Engineer, Northeast Agricultural University, Harbin, Heilongjiang, 150030, China; *Corresponding author: defuwang0203@sohu.com*

INTRODUCTION

With the improvement of the overall agricultural production capacity, the total production of crop straw in China exhibits a trend of increasing growth overall. At present, China is the world's largest producer of crop residue. In 2005, the total straw production reached 0.84 billion tons (Bi *et al.* 2010), which included about 0.25 billion tons of corn straw. Every year, large quantities of straw is burnt as waste; gases of PM2.5, SO_2, NOx, NH_3, CH_4, black carbon, organic carbon, volatile organic compounds, CO, and CO_2 released from plant residue burning cause environmental pollution (Cao *et al.* 2008). As the most abundantly available renewable resource on earth, rational utilization of residue can realize resource recycling, alleviate energy crisis, protect the global environment, and promote the sustainable development of both agriculture and economy (Chang *et al.* 2012).

Corn residue remaining after harvest incudes the stalk, leaf, husk, cob, and downed ears. The stalk represents almost 27.5% of the corn plant. The corn stalk consists of the rind and pith. The main components of the rind are cellulose and xylogen, which provide high intensity and good toughness; they are excellent raw materials in papermaking and artificial boards, *etc.* (Sun and Guo 2001). The pith of corn stalk, being rich in nutrients crude protein, crude fat and sugar, is an excellent feed for ruminants.

Separation of the pith and rind will greatly improve the applicability of corn stalk, in order to achieve the best use of each component. Each part of corn stalk must be effective separation for the most effective utilization of corn stover resources. Before straw resources can be used effectively, they must be preprocessed by smashing and segregating their skins, cores, and leaves. Preprocessing represents 33% of the total energy consumption during straw processing (Wooley *et al.* 1999). Due to the huge straw resources, how to reduce energy consumptions in straw resources processing is a main issue of straw resource recycling, which must be studied. Most studies in this area concentrate on the energy consumed during straw chopping or smashing (Schell and Harwood 1994; Wu *et al.* 2001; Zhang *et al.* 2003; Mani *et al.* 2004, 2006; AnBitra *et al.* 2009).

Currently, there are no reports on energy consumption related to the separation of corn stalk rind and pith. The objective of this paper is to examine power consumption during rind and pith reparation on a self-designed experimental platform. Moreover, the working parameters of the separating mechanism were optimized for energy conservation and production efficiency improvement.

EXPERIMENTAL

Materials

Xiangfang Test Base of Northeast Agricultural University provided corn stalks. Their geometrical parameters were as follows: average diameter of roots, 28.25 mm; average diameter of the top, 10.68 mm; and average length, 2,800 mm. The moisture content of straws (excluding leaves) was 12.4% (with a standard deviation of 0.011). Comparatively intact straws were selected and cut into two semi-straws approximately along the axis of corn straw, and their leaves were removed.

Experiment Device Structure and Experimental Parameters

Pith-stripping tests were carried out on the self-designed experimental platform composed of a core scraping part, an extending-extrusion feeding part, and a measurement control system. The scraping part (Fig. 1) served as the core component of the entire device and consisted of a rotational pith-stripping roll and a mounting panel on its bottom. The extending-extrusion feeding part (Fig. 2) was formed by a pair of round rollers that rotate against each other and have alveolar ridge. During experiments, corn stalk was extended and extruded by the extending-extrusion feeding roll. Next, it was delivered to the clearance between pith-stripping and mounting panel of the core scraping part at a certain speed; as driven by dynamo, the pith-stripping performs rotational motions and the scraper installed on it separated the pith of corn stalk from the rind.

Thirty scraper blades in 5 groups were mounted on the pith-stripping roll in the circumferential direction, and there were 6 blades for each group. The length and thickness of those blades were 120 mm and 5 mm, respectively. Moreover, the cutting edges of different angles were milled on the working side of scraper blades; pictures of two scraper blades with different helix angles are shown in Fig. 3. The helix angle was similar to the spiral angle of cylindrical milling cutter. By referencing influences of the variation range of spiral angles of mill-cutter on service life and work stability (Zatarain *et al.* 2006; Sims *et al.* 2008; Pan *et al.* 2008; Song 2009), the helix angle of scraper blade was varied from 0 to 40°. The distance from cutting edge of the scraper blade to the mounting panel on its bottom is called the "tooth-panel clearance", and it has a significant impact on core scraping effects (Liu and Wang 2011; Chen *et al.* 2012). During tests, thickness for the upper rind of corn stalk is 0.5 to 0.8 mm, while 1.0 to 1.5 mm for the middle and 1.5 to 1.8 mm for the root. To guarantee the integrity and the scraping rate of stalk skin after core scraping (Wang *et al.* 2012) after trial tests, the tooth-panel clearance ranged from 1 to 5 mm during experiments.

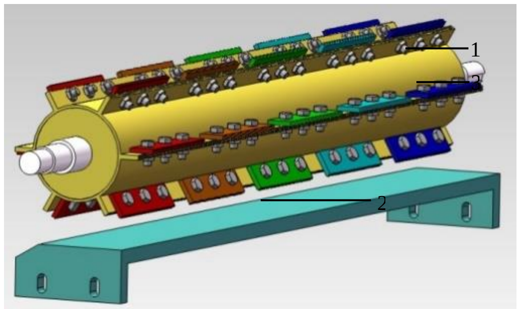

Fig. 1. Core scraping parts: 1. Pith-stripping roll; 2. Mounting panel; and 3. Scraper blade

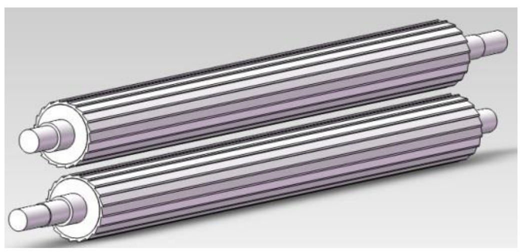

Fig. 2. Extending-extrusion feeding parts

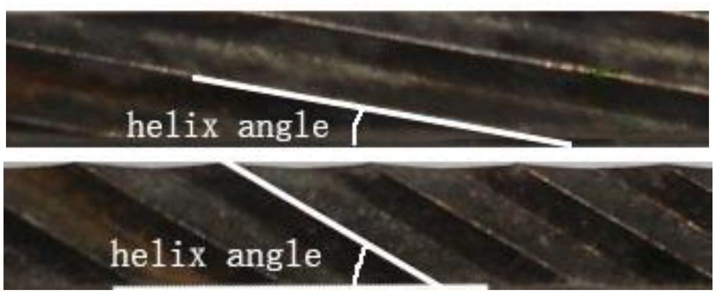

Fig. 3. Two scrapers with different helix angles

Table 1. Experiment Design

Horizontal	Experimental Factors			
	Rotational Speed A (r·min^{-1})	Feeding Speed B (r·min^{-1})	Tooth-Panel Clearance *C* (mm)	Helix Angle *D* (°)
-2	210	177	1	0
-1	420	236	2	10
0	630	295	3	20
1	840	354	4	30
2	1050	413	5	40

During experiments, the pith-stripping roll and the extending-extrusion feeding roll were separately driven by two independent motors, which were connected to two different inverters so that rotational speeds could be adjusted independently to conduct the corresponding operations. The rotational speed of the pith-stripping roll varied between 210 r/min and 1050 r/min, and the operating frequencies of the corresponding motor was between 10 Hz and 50 Hz. By comparison, the rotational speed for the extending-extrusion feeding roll varied from 177 r/min to 413 r/min (Liu and Wang 2011), and the corresponding motor operating frequencies were 9 Hz and 21 Hz. The experimental process used an orthogonal design (Table 1).

Acquisition of Experimental Data

A special measurement control system was employed to conduct data measurement and acquisition during the experiments, as well as to adjust and control operating parameters of the equipment. The electric energy consumed by the core scraping mechanism can be divided into two parts. One is the power consumption when the system has no load; the other is consumed when core scraping parts conduct rind and pith separation of corn stalk. The electric power difference method was adopted by this measurement control system to indirectly measure the electric energies consumed by the core scraping parts. The total electric energy consumed by core scraping activities of the mechanism is the sum of power consumptions generated by no-load core scraping device and electric energies consumed by core scraping (Cadoche and López 1989; Holtzapple *et al.* 1989; Dong *et al.* 2012; Chen *et al.* 2012); that is,

$$P_t = P_k + P_e \tag{1}$$

Therefore, electric energies consumed by core scraping can be calculated according to the equation below,

$$P_e = P_t - P_k \tag{2}$$

where P_t (Wh) refers to the total power consumption of the core scraping operations, P_k (Wh) is the power consumption for the no-load core scraping device, P_e (Wh) is the power consumption generated by core scraping, which is the electric power generated by separating the core from the straw skin.

With respect to the no-load operation of core the scraping device, power consumption P_k mainly includes inverter losses, dynamo losses, the no-load consumptions of pith-stripping roll, mechanical losses of core scraping device and losses of other parts, *etc.* In the case of no load, the power dissipation, P_k, was acquired by the measurement control system. The electric power difference method features anti-interference ability, high reliability, and strong universality and lacks structural constraints.

The structure of the measurement control system is presented in Fig. 4. The system was comprised of inverters, AC current transformer, measurement instrument, rotational speed sensors, and a micro-computer. The measuring instrument measured power consumption of the core scraping experiment platform during its operation as well as acquired rotational speeds of pith-stripping roll and feeding roll by means of a rotational speed sensor connected to their axes. In addition, the measuring instrument conveyed data to the computer with a USB interface of 485 in real time; the corresponding data acquisition frequency was 16 Hz.

Data communication protocols of various interfaces were the standard MODBUS-RTU protocol. Electrical signals, such as power dissipations and rotational speed, were converted into digital signal and transmitted to microcomputer through a 485-USB convertor, and thus, the real-time measurement for electric powers consumption of a core-scraping device was achieved.

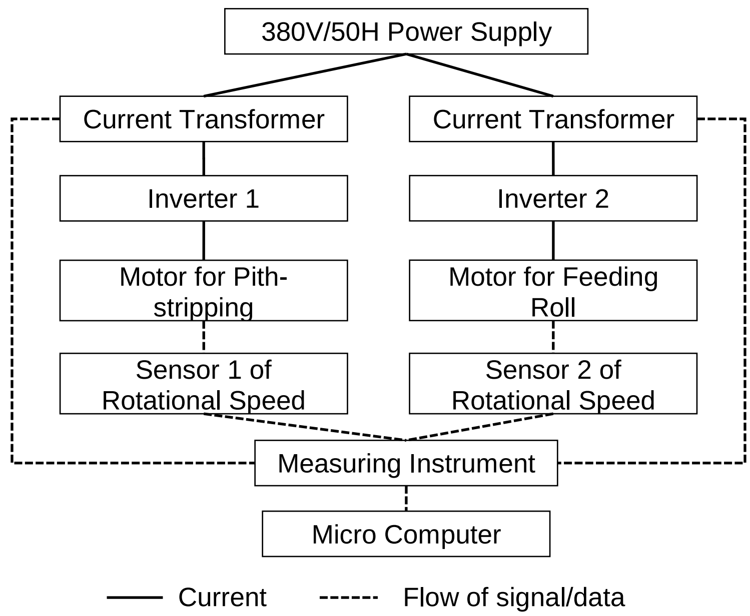

Fig. 4. Measurement control system diagram of pith stripping

Evaluation Indexes and Data Analysis

As differences in lengths and diameters of every corn stalk give rise to various qualities, electric energies consumed during core scraping must be diverse. In order to eliminate influences of those differences on experimental results, these results are more comparable. In this paper, the specific energy (Mani *et al.* 2006; AnBitra *et al.* 2009) is adopted as an evaluation index in the case that levels of experimental parameters are different. Concerning specific energy, it refers to energies consumed by core scraping device which processes stalk of unit mass and its unit is $Wh \cdot kg^{-1}$. A digital scale, whose capacity and readability are 3200 g and 0.01 g, respectively, weights the mass of corn stalk. For every group of experiment, at least 8 stalks are used and the core scraping power dissipation of each stalk is measured; in the end, an average value that has been figured out is treated as the measurement result.

There are three evaluation parameters based on the specific energy.

(1) Effective Specific Energy (ESE) refers to the electric energy consumed by processing corn stalks of unit mass and it can be defined as follows,

$$E_e = P_e / m \tag{3}$$

where E_e is the ESE ($Wh \cdot kg^{-1}$), and m is the mass of processed stalk (kg).

(2) Total Specific Energy (TSE) refers to the total electric energy consumed by the core scraping device used to process corn stalk of unit mass,

$$E_t = P_t / m \tag{4}$$

where E_t is the TSE ($Wh \cdot kg^{-1}$).

(3) Energy Utilization Ratio (EUR) refers to the ratio of ESE and TSE,

$$\rho = E_e / E_t = P_e / P_t = 1 - P_k / P_t \quad (5)$$

where ρ is the EUR (%).

The ESE is used to do effective work; in other words, it is the power consumed by scraping stalk cores from the skin. Besides the effective work, TSE also measures circuit power losses at the time of device operations and the power consumed by rotating members due to mechanical wear. A larger ρ indicates higher mechanical efficiency. Equation 5 shows that ρ can be improved by reducing the idle power consumption P_k.

RESULTS AND DISCUSSION

The ESE, TSE, and EUR served as evaluation indexes to perform orthogonal tests for 4 experimental factors. The response surface method was adopted to carry out data processing by using the Design Expert 8 software (Stat-Ease, Minneapolis, MN, USA), so as to obtain the influence law of experimental factors on evaluation indexes.

No-load Energy Consumption

For the purpose of ESE calculation, the power consumption of the core scraping part under the circumstance of no load must be considered. In such a condition, no-load powers of those parts were respectively recorded according to 5 different rotational speeds performed by the pith-stripping from 210 rpm to 1,050 rpm. In addition, the plot of rotational speed *versus* the no-load consumption showed a linear relationship between them (Fig. 5). With the increase in rotational speed, power consumption was mainly derived from the work caused by the increase in rotational speed of pith-stripping roll while torque remains unchanged. In Fig. 5, the intercept of 124.8 W could be regarded as the power consumption from circuits of the entire measurement control system itself.

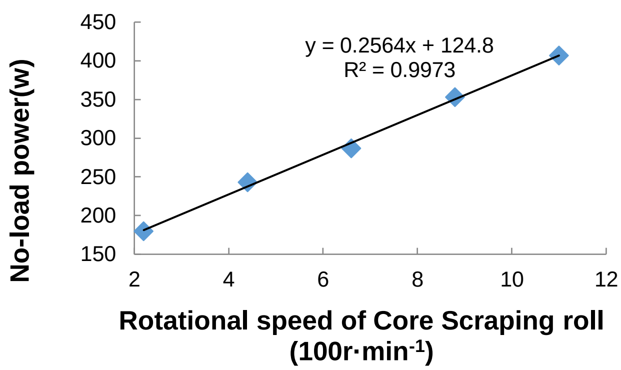

Fig. 5. Energy consumption variations with the change in rotational speed in no-load conditions

F-test for ESE E_e

According to the ANOVA analysis in Table 2, the *P*-value of the model is less than 0.0001, which indicates that the model is highly significant. The determination coefficient R^2 of this model (0.9695) indicates that this model has a favorable fitting degree and a small experimental error. Because the model showed no significant lack of fit (p = 0.8422 > 0.1), it was an appropriate model. As a result, the model could be used to evaluate the influence law of various experimental factors on the core scraping mechanism. For all of the model variables, all monomial terms of the model were significant, while quadratic terms of (B^2) and (C^2) together with the cross term (AC, BC, BD, CD) were also significant. The ESE varied between 0.5 and 2.0 Wh·kg^{-1}. The regression model contained monomial terms, quadratic terms, and cross terms (Eq. 6).

$$E_e=1.17+0.30A-0.17B-0.24C+0.054D+0.023AB-0.12AC-4.942E-003AD-0.074BC-0.062BD-0.064CD-0.038A^2+0.049B^2+0.068C^2-0.001967D^2 (R^2=0.9695) \quad (6)$$

Based on absolute values of the coefficients of linear entries of this model, the sequence for 4 factors influencing the ESE was $A > C >$ B $> D$; that is, rotational speed of pith-stripping roll > tooth-panel clearance > feeding speed > helix angle of scraper blade.

Table 2. Variance Analysis for Regression Model of ESE

Model Item	Mean Square Error	*F*-Value	*P*-Value
Model	0.36**	34.09	< 0.0001
A-Rotational Speed	2.23**	209.86	< 0.0001
B-Feeding Speed	0.68**	64.36	< 0.0001
C- Clearance	1.39**	130.61	< 0.0001
D- Helix Angle	0.070*	6.60	0.0214
AB	0.00875	0.82	0.3788
AC	0.22**	21.16	0.0003
AD	0.000391	0.037	0.8505
BC	0.087*	8.15	0.0121
BD	0.061*	5.74	0.0300
CD	0.065*	6.08	0.0262
A^2	0.040	3.73	0.0725
B^2	0.067*	6.31	0.0239
C^2	0.13**	11.96	0.0035
D^2	0.00011	0.00998	0.9217
Lack of Fit	0.00789	0.49	0.8422

Notes: ** coefficients significant at 99%; * coefficients significant at 95%.

Table 3. Variance Analysis for Regression Model of TSE

Model Item	Mean Square Error	F Value	P Value
Model	10.10**	19.47	< 0.0001
A- Rotational Speed	76.68**	147.87	< 0.0001
B- Feeding Speed	34.10**	65.75	< 0.0001
C- Clearance	3.54*	6.83	0.0195
D- Helix Angle	1.77	3.42	0.0844
AB	0.48	0.94	0.3489
AC	0.80	1.54	0.2335
AD	0.20	0.38	0.5469
BC	0.75	1.45	0.2473
BD	1.08	2.08	0.1696
CD	2.07	3.99	0.0642
A^2	1.59	3.07	0.1004
B^2	13.40**	25.84	0.0001
C^2	0.15	0.28	0.6020
D^2	3.42*	6.59	0.0214
Lack of Fit	0.55	1.22	0.4358

Notes: ** coefficients significant at 99%; * coefficients significant at 95%.

F-Test for TSE E_t

According to the ANOVA analysis (Table 3), the *P*-value of the model is less than 0.0001, which indicates that the model is highly significant. The determination coefficient R^2 of this model is 0.9479, which means that this model has a favorable fitting degree and a small experimental error. As a result, the model could be used to evaluate the influence law of various experimental factors on the TSE. For all items of this model, rotational speed (*A*), feeding speed (*B*), clearance (*C*), quadratic feeding speed (B^2), and quadratic blade angle (D^2) were all significant and had great influences on the TSE; by contrast, impacts of the helix angle (*D*) of scraper blade on the TSE were not significant. Variation range of the TSE was between 4 and 13.0 Wh·kg^{-1}. The corresponding regression model is shown as Eq. 7.

$$E_t=7.89+1.79A-1.19B-0.38C-0.27D-0.17AB-0.22AC-0.11AD-0.22BC-0.26BD-0.36CD-0.24A^2+0.70B^2-0.073C^2+0.35D^2 (R^2=0.9479) \quad (7)$$

Based on the absolute value of the coefficients of linear entries of this model, it was clear that the sequence for 4 factors influencing the TSE was $A > B > C > D$; that was, rotational speed of a pith-stripping roll > feeding speed > tooth-panel clearance > helix angle of scraper blade.

Table 4. Variance Analysis for Regression Model of EUR

Model Item	Mean Square Error	F Value	P-Value
Model	15.82**	18.37	<0.0001
A- Rotational Speed	11.85**	13.76	0.0021
B- Feeding Speed	0.74	0.86	0.3696
C- Clearance	109.67**	127.33	<0.0001
D-Helix Angle	25.16**	29.21	<0.0001
AB	6.94*	8.06	0.0125
AC	5.11*	5.93	0.0278
AD	0.32	0.37	0.5500
BC	10.24**	11.88	0.0036
BD	0.37	0.43	0.5211
CD	0.55	0.64	0.4362
A^2	1.72	2.00	0.1781
B^2	8.71**	10.11	0.0062
C^2	23.23**	26.97	0.0001
D^2	10.41**	12.09	0.0034
Lack of Fit	1.01	1.80	0.2676

Notes: Parameter coefficients marked with ** were at a significant level of 99%; while those marked with * were at a significant level of 95%.

F-test for EUR ρ

According to the ANOVA analysis (Table 4), the *P*-value of the model is less than 0.0001, which indicates that the model is highly significant. Determination coefficient R^2 of this model is 0.9449, which means that the model had a favorable fitting degree and a small experiment error. As a result, the model could be used to evaluate the influence law of various parameters on the EUR of core scraping mechanism. For all items of this model, rotational speed (*A*), clearance (*C*), and the helix angle of blade (*D*) were all significant and had great influences on the EUR. In contrast, impacts of feeding speed on this ratio were not significant. Depending on experimental data, the value range of the EUR was between 11% and 24%. The corresponding regression model is shown as Eq. 8.

$$\rho=14.78+0.70A-0.18B-2.14C+1.02D+0.66AB-0.57AC-0.14AD-0.80BC-0.15BD-0.19CD-0.25A^2-0.56B^2+0.92C^2-0.62D^2 (R^2=0.9449) \quad (8)$$

Based on the absolute value of the coefficients of linear entries of this model, it was clear that sequence for 4 factors influencing the ratio between net and total power consumptions was $C > D > A > B$; that was, tooth-panel clearance > helix angle of scraper blade > rotational speed of a pith-stripping roll > feeding speed.

Law of Single Factor Influence

Influences of single factor on ESE

By setting other factors at a level of 0, the influence law curve of various single factors on the ESE could be drawn, as shown in Fig. 6. With the rotational speed of pith-stripping increasing from a level of -2 to +2, the average ESE of core scraping mechanism increased from 0.4 Wh·kg^{-1} to 1.6 Wh·kg^{-1} gradually. Together with the increase in rotational speed of this mechanism, the number of stalk scraping per unit time and the power dissipation consumed by core scraping both increased. Therefore, the increase in average ESE was basically consistent with previous descriptions (Liu 2009).

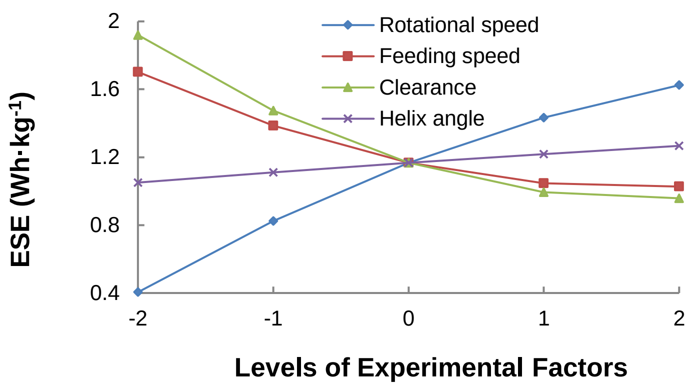

Fig. 6. Influence curves of various single factors on ESE

As the helix angle became larger, the average ESE of the core scraping mechanism moderately increased from 1.05 Wh·kg^{-1} to 1.3 Wh·kg^{-1}. Thus, the influence of the scraper blade helix angle on ESE was insignificant, which conformed the ANOVA results given in Table 2. The working process of this mechanism was similar to a milling process. According to the mathematical model of cutting force, although the increase in spiral angle of a miller could enlarge their cutting forces (Pan *et al.* 2008), such an enlargement would be insignificant (Xu and Zhang 2009). Moreover, forces required by cutting stalk cores were far smaller than metal cutting forces, and changes in the helix angle of a scraper blade failed to change the cutting force in a remarkable way. As a result, changes in this helix angle did not significantly affect the ESE.

With increases in the feeding speed and the tooth-panel clearance, the average specific energy of the core scraping mechanism decreased from 1.70 Wh·kg^{-1} to 1.02 Wh·kg^{-1}, and 1.92 Wh·kg^{-1} to 0.96 Wh·kg^{-1}, respectively. The corresponding reason was that, when the rotational speed of a pith-stripping was fixed, the number of core scraping per unit length decreased with the increase in feeding speed, this might cause the ESE reduction. In addition, with the enlargement of clearance, the depth into which a scraper blade cut the stalk core dropped so that the work that could be done reduced inevitably and the ESE reduced.

Influences of single factor on TSE

As shown in Fig. 7, changes in the rotational speed of pith stripping roll and the feeding speed had a significant influence on the TSE. As the rotational speed of pith-stripping went up from a level of -2 to +2, the average TSE substantially increased from 3.35 Wh·kg^{-1} to 10.50 Wh·kg^{-1} with a rate of growth of 213%. In the case that rotational speed of pith-stripping rose, more power should have been consumed to accelerate such a rotational speed on one hand, the number of core scraping increased due to the acceleration of this rotational speed so that the ESE also went up. As a result, the TSE increased.

With the increase in feeding speed, the average TSE was reduced from 13.07 Wh·kg^{-1} to 8.30 Wh·kg^{-1}. While feeding speed accelerated, core scraping time for a single straw decreased. Hence, both the electric energy consumed and TSE decreased, which was consistent with previous results (Chen *et al.* 2007).

Concerning clearance and helix angle, their influences on the TSE were not significant. When the tooth-panel clearance increased, the average TSE reduced from 8.36 Wh·kg^{-1} to 6.82 Wh·kg^{-1}, mainly caused by the reduction in ESE, given by the enlargement of this clearance. While the clearance had a significant influence on the ESE (Fig. 6), the influence of tooth-panel clearance on the TSE was insignificant, as the percentage taken by the ESE in the TSE was rather low. If the helix angle of a scraper blade increased, the average TSE dropped from 9.84 Wh·kg^{-1} to 8.75 Wh·kg^{-1}. The helix angle had an insignificant influence on ESE, so did its influence on the TSE.

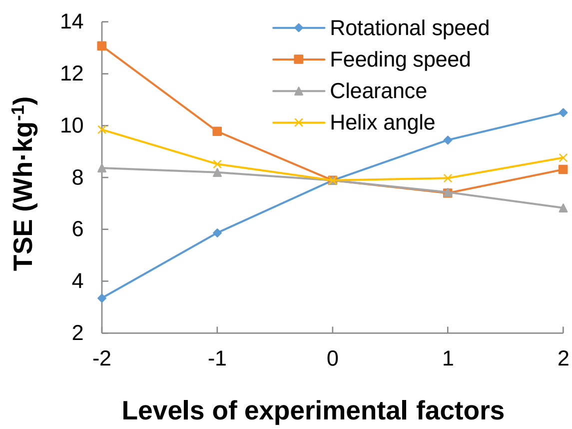

Fig. 7. Influence curves of various single factors on TSE

Influences of single factor on EUR

Factors that had a significant influence on EUR were tooth-panel clearance and helix angle of scraper. Within the scope of experimental factors, levels of other factors were set to be 0, and the EUR reduced from 22.7% to 14.2% along with the increase in tooth-panel clearance. Moreover, along with clearance increase, depth into which the scraper blade cut the stalk core decreased, this lead to the decreasing of the scraping area and width; as a result, cutting force was diminished (Liu *et al.* 2007). This phenomenon conformed to the experimental results of wood scraping (Chen *et al.* 2007). As the reduction in cutting force could give rise to the corresponding reduction in net power consumptions generated by core scraping in an inevitable way, the EUR drops. However, with the increase in helix angle of a scraper blade, both the cutting force (Pan *et al.* 2008) and the net power consumption from core scraping also increased so that the EUR increased from 10.3% to 14.3%.

When feeding speed was accelerated (slowed down), processing time for straws was shortened (increased), correspondingly, and the ESE and TSE of the core scraping mechanism dropped (went up), simultaneously. Hence, variations of feeding speed had an insignificant influence on the EUR (Fig. 8). Similarly, increases (decreases) in the rotational speed of pith-stripping could make both idle energy consumption and core scraping energy consumption rose (went down) at the same time. Therefore, the influence of pith-stripping rotational speed on the EUR was not significant.

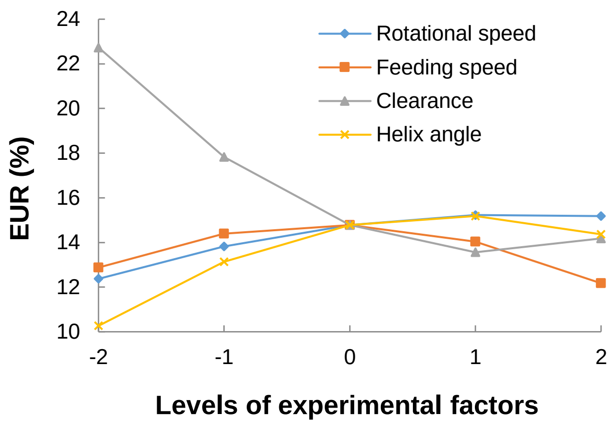

Fig. 8. Influence curves of various single factors on EUR

Response Surface Analysis

In order to analyze interactions among all influence factors, response surfaces were drawn to carry out intuitive analysis. By setting levels of different factors at 0, respectively, interaction surfaces sand contour maps could be obtained for another two factors. Below, several experimental factors with rather significant interactions were selected to perform response surface analysis for the ESE, TSE, and the EUR.

Response surface analysis for influence of experimental factors on ESE

According to the ANOVA analysis in Table 2, influences of cross terms were significant, such as the rotational speed of pith-stripping and tooth-panel clearance, the feeding speed and tooth-panel clearance, the feeding speed and helix angle, the tooth-panel clearance and helix angle, *etc.* As a result, analysis was focused on these four groups. Based on Fig. 9a, with the increase in rotational speed of pith-stripping and the reduction in tooth-panel clearance, the ESE of core scraping mechanism went up, which meant that more energies were consumed by core scraping. Based on Fig. 9b, with increases in both the tooth-panel clearance and the feeding speed, consumption of the ESE diminished for the core scraping mechanism. The corresponding reasons were that the number of core scraping in unit length increased together with the acceleration of feeding speed, and the depth at which scraper blade entered the stalk core decreased, giving rise to reduction in cutting force. Hence, net power consumption generated by core scraping decreased so that the ESE was reduced. Based on Fig. 9c, with reduction in feeding speed, the ESE slightly dropped with the increase in helix angle of blade at first and then went up substantially. In the case that feeding speed was rather low, larger helix angle should be selected to improve the ESE; in contrast, when feeding speed was low, small helix angle could be selected to improve it. However, to improve working efficiency during actual operations, feeding speed should not be too low in general cases; therefore, a scraper blade with very large helix angle was inappropriate and unfavorable. Based on Fig. 9d, with the reduction in tooth-panel clearance, ESE slightly went down and then significantly rose with the increase in helix angle, and higher ESE occurred when the tooth-panel clearance was small and the helix angle was large.

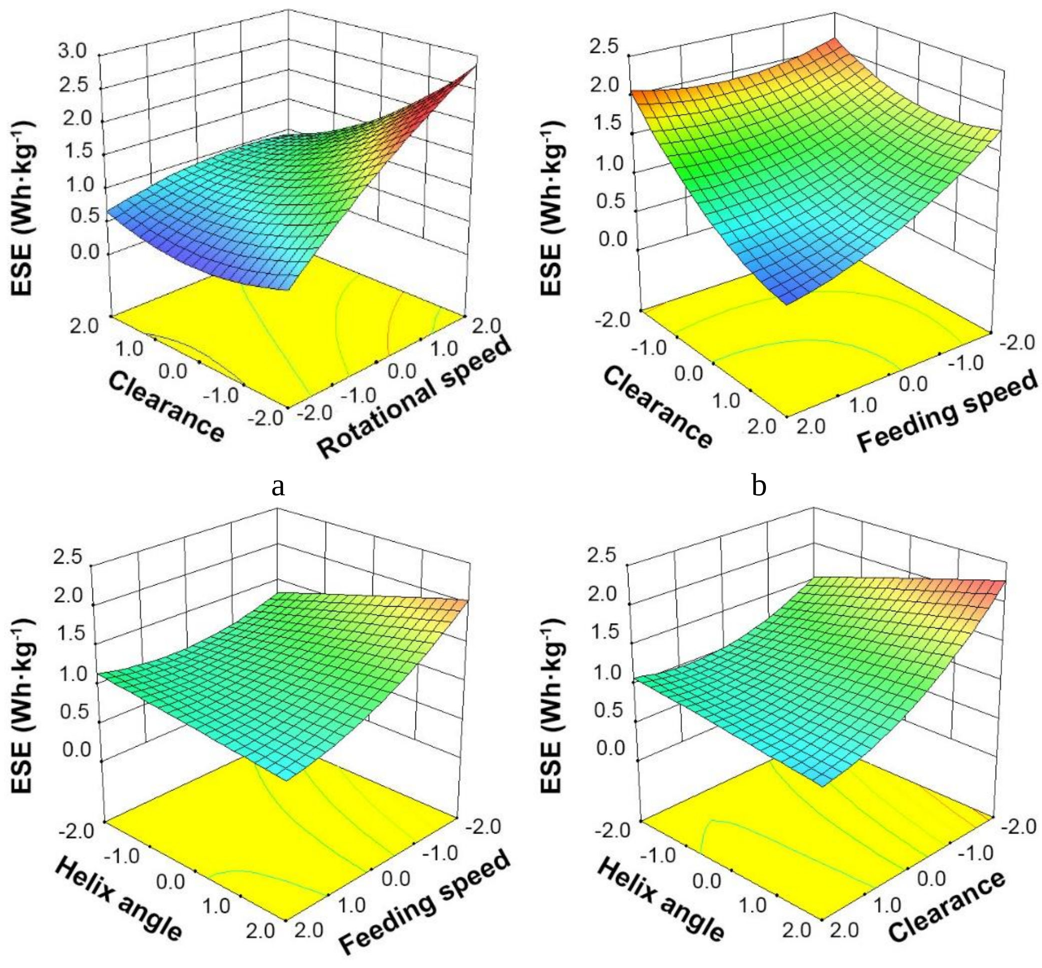

Fig. 9. Response surfaces of ESE**:** a. Interaction between rotational speed and clearance; b. Interaction between feeding speed and clearance; c Interaction between feeding speed and helix angle; d. Interaction between clearance and helix angle

Response surface analysis for influence of experimental factors on TSE

Figure 10 shows response surfaces of experimental factors *vs*. TSE and lists the two significant cross items response surfaces. Based on Fig. 10a, it was clear that with the gradual increase in helix angle, the total specific angle first slightly decreased and then substantially increased along with the reductions in feeding speed. When the helix angle was at a level of 0.8 and, at the same time, the feeding speed was at 1.0, the minimum value of TSE could be up to 7.20 Wh·kg^{-1}, and the core scraping mechanism worked in a state of energy conservation. Based on Fig. 10b, the TSE dropped with the reduction in rotational speed of pith-stripping, which was primarily caused by the no-load power consumption reductions of the core scraping mechanism. By contrast, the TSE of the pith-stripping mechanism slightly decreased, followed by a substantial increase with the decrease of feeding speed. When the feeding speed was roughly at a level of 1.0, the TSE was rather low, and the core scraping mechanism also worked in a state of energy conservation.

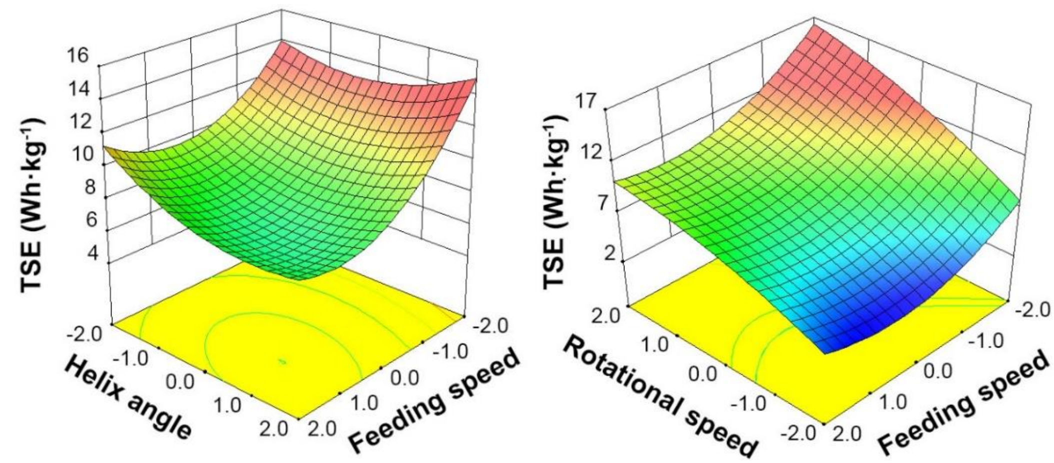

a b

a. Interaction between Feeding Speed and Helix Angle; b. Interaction between Rotational Speed and Feeding Speed

Fig. 10. Response surfaces of TSE

Response surface analysis for influence of experimental factors on EUR

Figure 11 shows response surfaces of experimental factors *vs.* EUR. With the increase in rotational speed of pith-stripping, the EUR firstly increased in a substantial manner and then went down with the reduction in feeding speed, which was gradually followed by a small rise and sharp decreased afterwards (Fig. 11a). Within the range of experimental factors, when the rotational speed of pith-stripping reached its maximum value and the feeding speed was approximately at a level of 0, the EUR was relatively high. In other words, energy consumption generated by core scraping took a large proportion in the total energy consumption, and the core scraping mechanism had a high mechanical efficiency. Figures 11b and 11c refer to influences of rotational speed *vs.* tooth-panel clearance and the feeding speed *vs.* tooth-panel clearance; their response surfaces both shared resemblances with the saddle shape and had similar influence on the EUR. When the tooth-panel clearance was rather large, the influence of rotational speed or feeding speed on the EUR were very small. When such a clearance decreased, EUR increased; the percentage of power dissipations consumed by core scraping was rather large, which signified that mechanical efficiency was relatively high. Based on Fig. 11d, with the increase in helix angle of a scraper blade, EUR firstly rose and then mildly declined along with the increase in rotational speed of pith stripping. The response surface showed that both the helix angle and the rotational speed of pith-stripping exerted certain interaction effects on the EUR. Specifically, when the helix angle of blade and the rotational speed reached a level of 0.5 and 1.0, respectively, the maximum EUR was acquired.

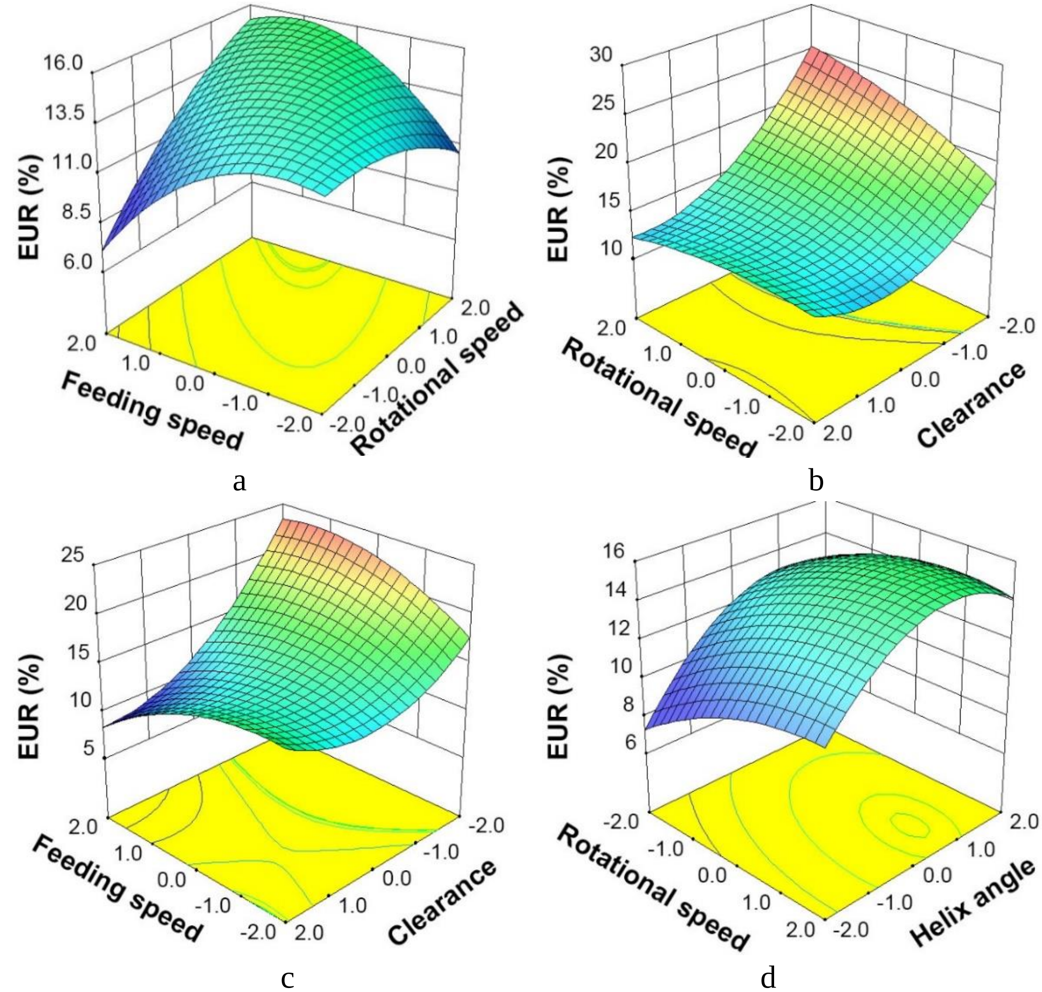

a. Interaction Between Feeding Speed and Rotational Speed; b. Interaction Between Rotational Speed and Tooth-panel Clearance; c. Interaction Between Feeding Speed and Tooth-panel Clearance; d. Interaction Between Rotational Speed and Helix Angle;

Fig. 11. Response surfaces of EUR

Experimental Parameter Optimization Based on Energy Consumptions

With regard to the core scraping mechanism, the higher the EUR, the higher the percentage taken by energies consumed by core scraping in the total energy consumption. In this case, the core scraping mechanism was able to achieve a high mechanical efficiency, which was one of the objectives for core scraping mechanism optimization. From the definition of EUR (Eq. 5), the no-load energy consumptions could be reduced by bringing down frictions among diverse parts and the moment of inertia of pith-stripping roll, *etc.* to improve the EUR.

In addition, during production practices, production efficiency was a factor, which was taken into account. The production efficiency of core scraping mechanism was determined by the feeding speed of extending-extrusion roll; a faster feeding speed resulted in higher production efficiency. Thus, high production efficiency was the second objective of experimental parameter optimization. Based on the above single factor and response surface analysis, core scraping effects of a core scraping mechanism were taken into a comprehensive account (Liu and Wang 2011) to perform ridge analysis for data using Design-Expert software. When the rotational speed of pith-stripping was at a level of 0.99, the maximum level for feeding speed was 2.00, the tooth-panel clearance was at a level of -1.44, helix angle of scraper blade at 0.50, ESE, TSE, and EUR were 2.21 $Wh \cdot kg^{-1}$, 10.73 $Wh \cdot kg^{-1}$, and 22.29%, respectively. Based on these parameters, verification tests were conducted. The results showed that the measured ESE, TSE, and EUR of the core scraping mechanism were 2.31 $Wh \cdot kg^{-1}$, 11.20 $Wh \cdot kg^{-1}$, and 23.51%, respectively, which conformed to predicted values within a confidence interval of 95%. Hence, the reliability of this model was verified.

This paper is based on corn stalk measurements at moisture content of about 12%. The effect of moisture content on energy consumption was not taken into consideration here, although it is one of the factors which will affect physical properties of the stalk, which might be one of the main points for our future studies.

CONCLUSIONS

1. Among the four factors selected in the experiment, the clearance between teeth and panel had significant effects on ESE and EUR. As a result, a reasonable clearance will achieve energy saving process for pith and rind separation.
2. Response surface analysis was carried out for energy consumptions from the core scraping mechanism on a self-designed core scraping experimental platform of corn stalks. The rotational speed of the pith-stripping roll, stalk feeding speed, tooth-panel clearance, and helix angle of the scraper blade were selected as experimental factors. The ESE, TSE, and EUR are adopted as evaluation indexes. On these bases, the influence of various factors on energy consumption generated by core scraping devices were analyzed. Within the range of experimental parameters, the obtained variation ranges for ESE, TSE, and EUR were 0.5 to 2.0 $Wh \cdot kg^{-1}$, 4.0 to 13.0 $Wh \cdot kg^{-1}$, and 11% to 24%, respectively.
3. On the basis of giving considerations to both the mechanical efficiency and the production efficiency of core scraping mechanism, the core scraping effects of an experimental platform were comprehensively considered to optimize the model. When the rotational speed of pith-stripping, feeding speed, tooth-panel clearance, and helix angle were 840 r/min, 413 r/min, 1.56 mm, and 25°, respectively, the EUR of this mechanism reached 22.29%, and the maximum production efficiency was achieved.

ACKNOWLEDGMENTS

The authors acknowledge the funding support of Specialized Research Fund for the Doctoral Program of Higher Education.

REFERENCES CITED

AnBitra, V. S., Womac, A. R., Igathinathane, C., Miu, P. I., Yang, Y. T., Smith, D. R., Chevanan, N., and Sokhansanj, S. (2009). "Direct measures of mechanical energy for knife mill size reduction of switchgrass, wheat straw, and corn stover," *Bioresource Technol.* 100(24), 6578-6585. DOI: 10.1016/j.biortech.2009.07.069

Bi, Y. Y., Wang, Y. J., and Gao, C. Y. (2010). "Straw resource quantity and its regional distribution in China," *Journal of Agricultural Mechanization Research* 32(3), 1-7.

Cadoche, L., and López, G. D. (1989). "Assessment of size reduction as a preliminary step in the production of ethanol from lignocellulosic wastes," *Biological Wastes* 30(2), 153-157. DOI: 10.1016/0269-7483(89)90069-4

Cao, G. L., Zhang, X. Y., Wang, Y. Q., and Zheng, F. C. (2008). "Estimation of emissions from field burning of crop straw in China," *Chinese Science Bulletin* 53(5), 784-790. DOI: 10.1007/s11434-008-0145-4

Chang, J., Liu, M., Yin, Q. Q., Zheng, Q. H., Guo, H. W., and Fan, C. G. (2012). "Progress of research on pretreatment of corn stover," *Chinese Agricultural Science Bulletin* 28(11), 1-8.

Chen, S. T., Zhou, X. J., Shi, Q. X., Liu, S. D., Pang, J., and Han, G. W. (2007). "Experiment and optimization on factors affecting the performance of wheat stalk macerator smashing devices," *Transactions of the Chinese Society for Agricultural Machinery* 38(9), 67-70.

Chen, Z. G., Wang, D., Li, L. Q., and Shan, R. X. (2012). "Experiment on tensile and shearing characteristics of rind of corn stalk," *Transactions of the Chinese Society of Agricultural Engineering* 28(21), 59-65. DOI: 10.3969/j.issn.1002-6819.2012.21.009

Dong, X., Liu, L. Y., Li, W. Z., Li, Z. H., Zhang, Y. W., and Zhang, H. Q. (2012). "Power consumption experiment of corn straw adjusting material device based on horizontal roller," *Transactions of the Chinese Society for Agricultural Machinery* 43(S1), 198-201. DOI: 10.6041/j.issn.1000-1298.2012.S0.039

Holtzapple, M. T., Humphrey, A. E., and Taylor, J. D. (1989). "Energy requirements for the size reduction of poplar and aspen wood," *Biotechnol. Bioeng.* 33(2), 207-210. DOI: 10.1002/bit.260330210

Liu, G. (2009). *Design and Experimental Study on Performance of Straw Rubber's Feeding Device*, Master's Thesis, Inner Mongolia Agricultural University, Hohhot, China.

Liu, L. L., and Wang, D. (2011). "Experimental study on separating mechanism of corn straw," *Journal of Northeast Agricultural University* 42(2), 43-47.

Liu, S. Y., Wang, X. H., and Dong, Z. W. (2007). "Numerical simulation for effect of cutting depth on Al-alloy cutting process," *Nonferrous Metals* 59(02), 32-34.

Mani, S., Tabil, L. G., and Sokhansanj, S. (2004). "Grinding performance and physical properties of wheat and barley straws, corn stover and switchgrass," *Biomass and Bioenergy* 27(4), 339-352. DOI: 10.1016/j.biombioe.2004.03.007

Mani, S., Tabil, L. G., and Sokhansanj, S. (2006). "Specific energy requirement for compacting corn stover," *Bioresource Technol.* 97(12), 1420-1426. DOI: 10.1016/j.biortech.2005.06.019

Pan, Y. Z., Ai, X., Tang, Z. T., and Zhao, J. (2008). "Optimization of tool geometry and cutting parameters based on a predictive model of cutting force," *China Mechanical Engineering* 19(4), 428-431.

Schell, D. J., and Harwood, C. (1994). "Milling of lignocellulosic biomass," *Applied Biochemistry and Biotechnology* 45(1), 159-168. DOI: 10.1007/BF02941795

Sims, N. D., Mann, B., and Huyanan, S. (2008). "Analytical prediction of chatter stability for variable pitch and variable helix milling tools," *Journal of Sound and Vibration* 317(3–5), 664-686. DOI: 10.1016/j.jsv.2008.03.045

Song, Q. H. (2009). *High-Speed Milling Stability and Machining Accuracy*, Ph.D. Dissertation, ShanDong University, Jinan, China.

Sun, Z. Y., and Guo, S. M. (2001). "Husk and stalk separation and pulping experiment of corn straw," *China Pulp & Paper Industry* 22(5), 41-42.

Wang, D., Chen, Z. G., and Yu, K. Q. (2012). "Parameter optimization on separating mechanism for rind and pith of corn straw," *Transactions of the Chinese Society for Agricultural Machinery* 43(10), 90-94. DOI: 10.6041/j. issn.1000-1298.2012.10.016

Wooley, R., Ruth, M., Sheehan, J., Ibsen, K., Majdeski, H., and Galvez, A. (1999). *Lignocellulosic Biomass to Ethanol Process Design and Economics Utilizing Co-current Dilute Acid Prehydrolysis and Enzymatic Hydrolysis: Current and Futuristic Scenarios* (Report No. NREL/TP-580-26157), National Renewable Energy Laboratory, Golden, CO, USA.

Wu, Z. Y., Gao, H. W., and Zhang, J. G. (2001). "Study on cutting velocity and power requirement in a maize stalk chopping process," *Transactions of The Chinese Society of Agricultural Machinery* 32(2), 38-41.

Xu, C. T., and Zhang, C. (2009). "A study on milling forces in high speed milling," *Electro-Mechanical Engineering* 25(1), 58-60.

Zatarain, M., Muñoa, J., Peigné, G., and Insperger, T. (2006). "Analysis of the influence of mill helix angle on chatter stability," *CIRP Annals - Manufacturing Technology* 55(1), 365-368. DOI: 10.1016/S0007-8506(07)60436-3

Zhang, H. X., Liu, S. D., Shi, Q. X., and Ni, C. A. (2003). "Influence of macerator," *Journal of Henan University of Science and Technology (Natural Science)* 24(02), 1-4. DOI: 10.15926/j .cnki .issn1672 -6871.2003.02.001

Article submitted: July 5, 2016; Peer review completed: September 4, 2016; Revised version received and accepted: September 10, 2016; Published: January 5, 2017.
DOI: 10.15376/biores.12.1.1300-1316